

Pressed roofing tile based on cementitious material and basalt powder: Technological and toxicological characterization

<http://dx.doi.org/10.1590/0370-44672022750028>

Franciele B. T. de Jesus^{1,3}

<https://orcid.org/0000-0001-7164-1938>

Kamila R. da Silva^{1,4}

<https://orcid.org/0000-0002-7934-7837>

Jordana M. Inocente^{1,5}

<https://orcid.org/0000-0002-9164-2660>

Carlos P. Bergmann^{2,6}

<https://orcid.org/0000-0002-8951-8943>

Sabrina Arcaro^{1,7}

<https://orcid.org/0000-0002-0668-7689>

Oscar R. K. Montedo^{1,8}

<https://orcid.org/0000-0002-3350-6732>

¹Universidade do Extremo Sul Catarinense – UNESC, Laboratório de Cerâmica Técnica, Criciúma – Santa Catarina – Brasil.

²Universidade Federal do Rio Grande do Sul – UFRGS, Escola de Engenharia, Programa de Pós-graduação em Engenharia de Minas, Metalúrgica e de Materiais, Porto Alegre - Rio Grande do Sul – Brasil.

E-mails: ³franburato@gmail.com,

⁴engenheirakamila@gmail.com,

⁵jordanainocente@gmail.com, ⁶bergmann@ufrgs.br,

⁷sarcaro@unesc.net, ⁸okm@unesc.net

Abstract

This study aims to develop a pressed concrete roofing tile from powder technology containing basalt powder in substitution of fine sand (aggregate) for application in building covers. Specimens were submitted to technological and toxicological characterization. Hence, pressed specimens based on cement and basalt powder were analyzed. In the bending strength test, the pressed samples containing a cement:basalt mass ratio of 1:6, water content of 5% and specific pressure of 25 MPa revealed a value of 3.82 ± 0.46 MPa at 28 days of curing, while the molded samples (reference) with cement:sand mass ratio of 1:5 and 15% water content revealed 1.72 ± 0.86 MPa. This composition, containing cement and basalt powder, is not toxic, confirming the possibility for total replacement of sand by basalt powder. Thus, it was demonstrated that the technical viability for the proposed process and the use of basalt powder to obtain pressed flat concrete roof tile meets technical requirements and standards, compared to conventional concrete roofing tiles.

Keywords: composites; pressing; strength; microstructure; roofing tile.

1. Introduction

The concrete roofing tiles are used for various roofs, with rectangular shape and wavy or flat profile, formed by cement, aggregate, water, and optionally, additives and pigment or surface coating (Damasceno *et al.*, 2015). When compared to ceramic tiles, concrete roofing tiles have similarities such as weight and diversity of colors. The importance of this tile has evolved in such a way that the Brazilian Association of Technical Standards (ASSOCIAÇÃO BRASILEIRA DE NORMAS TÉCNICAS) has developed standards to regulate the quality standards and properties of this product by means of NBR 13858 (ASSOCIAÇÃO BRASILEIRA DE NORMAS TÉCNICAS, 2009a).

The first concrete roofing tiles factory began production around 1976 in the city of São Paulo (Cabral Júnior *et al.*, 2019). Between 1970 and 1980, concrete roofing tile factories were also installed in the southern region, mainly in Santa Catarina. In 2018, production in São Paulo was distributed in 51 industrial plants, with a production of approximately 560 million m², corresponding to 70% of the total concrete roofing tiles manufactured in Brazil, while the South represents 18% of production and the Northeast 12% (Cabral Júnior *et al.*, 2019).

A comparative Life Cycle Assessment of ceramic versus concrete roof tiles in the Brazilian context has shown that ceramic tiles appear to have less impact than concrete tiles on Climate Change, Resource Depletion and Water Withdrawal (Souza *et al.*, 2015). However, the difference between the two alternatives was considered too low to be considered significant.

Since the ceramic industry generates a great impact on the environment, be it physical, chemical, and biological, produced by high energy consumption during the firing process, this industry becomes a major consumer of energy, providing emission of carbon dioxide (CO₂) and other gases and particulate materials rich in metals and other pollutants to the environment. On the other hand, the production of the most common binder used in concrete production, Portland cement, also generates a great impact, considering that in its production, approximately 844 kg of CO₂ are generated for each ton of produced clinker, making the cement industry responsible for 7% of global CO₂ emissions (Koppe *et al.*, 2015).

However, many initiatives have searched to reduce the environmental impact. Sam *et al.* [6] studied the feasibility

of using waste oils as blended binder to produce environmentally friendly roofing tiles. They used a blended binder composed of waste engine oil and waste vegetable oil with sand aggregate and fly ash to produce an innovative building material named WEV-Roofing tiles. They obtained roofing tiles with relatively lower embodied carbon and energy, which were 0.30 kg CO₂/equivalent and 0.55 MJ/kg, respectively.

In the search for the reduction of this impact, the incorporation of alternative materials, such as by-products of extractive processes of raw materials, in mortar compositions and the consolidation of cold material, through the reduction of energy consumption and CO₂ emission, has provided numerous studies. In fact, many studies of concrete materials have been carried out from the incorporation of by-products from the extraction and processing sector of ornamental rocks, such as elements of the compositions used (Destefani & Holanda, 2011).

In general, civil construction is responsible for the excessive consumption of natural resources from non-renewable sources, causing the need to extract these resources in large amounts from nature (Brasileiro & Matos, 2015). According to Koppe *et al.* (2015), there is a diversity of minerals extracted from nature, such as ornamental rocks, basalt, and granite, which have no mass industrial application and require controlled environmental management.

Menezes *et al.* (2010) studied the use of electro-fused alumina production waste in ceramic bricks and roof tiles. They used up to 30 wt% of the waste into a ceramic composition. They stated that it is possible to add up to 20 wt% of the waste of a ceramic composition, fired at 1000 °C for ceramic bricks and roof tiles. Under these conditions, they obtained a linear shrinkage of 1.8%, a water absorption of 17%, and modulus of rupture of 6.5 MPa that are values considered acceptable for red ceramic.

Cota *et al.* (2015) investigated the mechanical properties of concrete tiles with waste glass aggregate. They concluded that either 7.5 or 15 wt% of waste glass may be used in concretes without deterioration of the mechanical properties and the durability with the alkali-silica reaction. According to them, the obtained results are quite significant because they indicate a clear path to design and manufacture new classes of sustainable materials

for tiles and semi-dry compounds.

Moreover, natural fibers have been used in roofing tiles. Abraham *et al.* (2016) developed coir-fibre cement composite roofing tiles. They found that a composite with a fiber volume of 10% presented the optimum composite, reducing the weight of the roofing tile and its cost. The average breaking load increase from 48 (0 vol% of fiber addition) to 60 kgf (10 vol% fiber addition).

Due to the processing characteristics, its extraction generates large amounts of by-products, often in a powdery way, which are deposited in the courtyards of mining companies. In the case of basaltic rocks, they are found in abundance in the earth's crust and the by-product generated from its processing can be used on a large scale, if applied to a high consumption product on the market, such as tile.

These by-products typically have non-uniform granulometric distribution. Thus, considering a cementitious artifact, for example, a large granulometric distribution by-product can help to diminish porosity, increasing mechanical strength and decreasing water absorption.

Mendes, Guerra and Morales (2016) observe that the mechanical performance of Portland cement is directly affected by basalt residue. A positive effect was observed for contents ranging from 2.5 to 5% in fine fraction weight.

Koppe *et al.* (2015) evaluated the potential use of basaltic rock powders as raw material to produce alternative cements. They concluded that the studied basalts presented potential to be used in the alkali-activation process in natural state. The basalt powder was used as-received, which makes it potentially eco-efficient.

Santana and Ferreira (2006) demonstrated the increase in mechanical strength due to partial substitution of fine aggregate by crushing residue, applied in the concrete artifacts industry. After tests performed on the different aggregate:cement ratios, a considerable increase in compressive strength was confirmed between 7 and 28 days. The adequate replacement content was shown to be around 40% for concrete used in the most prefabricated artifacts.

Silva *et al.* (2022) developed cementitious material-based plates for the construction system of panel slabs using powder technology to reduce the amount of concrete in the slab. In this study, sand was partially (58.1 wt%, C3) and totally

(C1) replaced by basalt powder. Cementitious plates were obtained by uniaxial pressing at different compaction pressures. The molded plates (M) using sand and cement were obtained as references. The bending strength at 28 days of curing was 2.50 ± 0.10 MPa, which is higher than that of the molded plates (1.94 ± 0.11 MPa). It was concluded that pressing and sand substitution by basalt reduced the linear expansion from $0.059\% \pm 0.003\%$ (M) to $0.042\% \pm 0.007\%$ (C3), reducing the risk

of cracking. The evaluation of the environmental impact showed the potential of replacing sand with basalt, thus reducing the cost of the material. Therefore, pressed plates with the total substitution of sand by basalt achieved better results related to the molded plates and demonstrated considerable potential for application in the civil construction industry.

Thus, a flat tile of pressed concrete could be produced, through the powder technology, but without the use of the fir-

ing step, replacing the fine aggregate (sand) by basalt powder, in order to reduce the environmental impact, increase the mechanical strength, and possibly reduce the production cost of the obtained material. In view of the above, this article presents the results of a study to obtain a basalt-containing concrete roofing tile obtained by pressing from powder technology. A technological and toxicological characterization was performed for application in building covers.

2. Materials and methods

2.1 Materials

The selection of materials was carried out according to the technical standards NBR 13858 (ASSOCIAÇÃO BRASILEIRA DE NORMAS TÉCNICAS, 2009a), applied to molded tiles, and NBR 15310 (ASSOCIAÇÃO BRASILEIRA DE NORMAS TÉCNICAS, 2009b), applied to the manufacturing process of tile by pressing. The water used in all stages

of the research was obtained directly from the local water supplier according to NBR 15900-1 (ASSOCIAÇÃO BRASILEIRA DE NORMAS TÉCNICAS, 2009c). We used Portland type commercial cement of initially high strength, CPV-ARI, which presents high reactivity. It is recommended for cement artifact industries, for assisting in the rapid deformation and handling of

pieces according to NBR 5733 (ASSOCIAÇÃO BRASILEIRA DE NORMAS TÉCNICAS, 1991); compressive strength can reach 26 MPa on the first day. The used fine aggregate (sand) is commercially used and has a fineness module of 1.8, a specific mass of 2.62 g/cm^3 , and a unit mass of 1.62 g/cm^3 . Basalt powder was supplied by Setep Construções S.A. (Brazil).

2.2 Characterization of basalt powder

The particle size distribution was determined by laser diffraction in a CILAS particle size analyzer, model PSA 1064. Chemical analysis was determined

by X-ray fluorescence (FRX, Panalytical, WRFDX AXIOS MAX model). Mineralogical analysis was performed by X-ray diffraction (XRD, Phillips, X'Pert MDP

model; $\text{CuK}\alpha$ radiation). The real density was performed by helium gas pycnometry (Quantachrome Instruments, model ULTRAPYC 1200e).

2.3 Definition of the cement: aggregate mass ratio

Considering that basalt powder is chemically and structurally different from sand, a preliminary study was necessary for the definition of the cement:aggregate mass ratio more appropriate for pressed specimens (PRE). For comparison, molded specimens (MOL) were prepared since there is no specific standard for this type of material (cement and basalt powder) and manufacturing process (pressing). The molded specimens (MOL, reference) were obtained with a cement:aggregate mass ratio of 1:5 and 15 wt.% of water.

The molding process was based on the NBR 7215 (ASSOCIAÇÃO BRASILEIRA DE NORMAS TÉCNICAS, 2019) standard

regarding the dimensions of the molds and the analyses to be applied. The water content was previously determined according to the consistency of the mortar, until reaching the appropriate point of molding and pressing for the size of the samples. This determination was made through tests in specimens with a water content of 5, 10, and 15 wt.% and it was verified which consistency presented the best result in the tests of mechanical bending strength (BS) in a universal mechanical testing machine EMIC (model 0555) and procedure according to NBR 12142 (ASSOCIAÇÃO BRASILEIRA DE NORMAS TÉCNICAS, 2010).

The pressures of 150, 160 and 180 bar

were applied, corresponding to the specific pressures of 25.5, 28.0, and 30.5 MPa, respectively, defined in preliminary tests. The cement:aggregate mass ratio of the PRE specimens was defined from the results of the BS test, as established by the experimental design. The adopted experimental design was 2^2 with central point in duplicate, considering two variables: specific pressure and cement:aggregate mass ratio of the mixture, as presented in Table 1, which were varied at two levels (-1 and +1). Six specimens were obtained for each cement:aggregate mass ratio. Only for T3 (central point), 12 specimens were prepared to improve the accuracy of the results, totaling 36 specimens.

Table 1 - Experimental design for defining the cement:aggregate mass ratio.

Cement: aggregate mass ratio	Specific Pressure (MPa)		
	25.5	28.0	30.5
1:5	T1		T2
1:6		T3	
1:7	T4		T5

Cement and basalt powder were mixed manually, humidified (5 wt.%)

and passed through a 200-mesh sieve to obtain adequate homogeneity and

granulation of the mixture. Each mixture was then uniaxially pressed

into an ICON hydraulic press (model 2X12-1.5) at the compaction pressures indicated in the experimental design. For MOL specimens, 15 units were prepared in a wooden mold (12 cm x 2 cm x 0.5 cm internal dimensions) with a standard cement:aggregate mass ratio for cement CPV-ARI: fine sand (1:5).

2.4 Evaluation of the effect of curing time on bending strength

Taking into account the best experimental condition obtained previously (cement:aggregate mass ratio and specific pressure), new PRE specimens were prepared to analyze the effect of the curing time on the BS at 7, 14, and 28 days, both for the PRE and MOL specimens.

The crystalline phases formed in the curing process were identified by X-ray diffraction (XRD, Phillips, X'Pert MDP model; CuK α radiation).

Porosity values were obtained from apparent and real densities. From the

This cement:aggregate mass ratio of MOL specimens is usually used in the manufacture of flat concrete tiles. The mixture was humidified (15 wt.%), homogenized, and molded. Afterwards, the PRE and MOL specimens were dried at room temperature for 24 h and then submitted to a submerged

weight and volume measurements of the specimens after the regularization of the faces, the apparent density (ρ_a) was determined. Five specimens of each experimental condition were measured with a caliper (Mitutoyo, model CD-81PSX). The real density (ρ_{real}) was obtained by the helium picnometry method (Quantachrome Ultrapyc 1200e).

The microstructure of the specimens was evaluated by scanning electron microscopy (SEM, Zeiss, EVO MA10 model) to analyze the pore distribution of the sample

cure in potable water, also at room temperature for 7 days. After this step, they were submitted to BS tests in a universal Mechanical Testing Machine EMIC (model CAL 0555) and procedure according to NBR 12142 (ASSOCIAÇÃO BRASILEIRA DE NORMAS TÉCNICAS, 2010).

and the microstructural features of the obtained materials.

The BS was determined according to NBR 13858 (ASSOCIAÇÃO BRASILEIRA DE NORMAS TÉCNICAS, 2009a) and NBR 15310 (ASSOCIAÇÃO BRASILEIRA DE NORMAS TÉCNICAS, 2010b) and performed in a Universal Mechanical Testing Machine (EMIC, model 0555). Each test specimen was chosen in such a way as to be apparently free of defects after immersion in water for 24 h.

2.5 Technological and toxicological characterization

With the best obtained results, new specimens were prepared under the same conditions mentioned in item 2.4, at 7, 14 and 28 days of curing, for characterization.

Water absorption was determined according to NBR 13858 (ASSOCIAÇÃO BRASILEIRA DE NORMAS TÉCNICAS, 2009a) for concrete tiles and NBR 15310 (ASSOCIAÇÃO BRASILEIRA DE NORMAS TÉCNICAS, 2009b). Five MOL specimens and five PRE specimens were used. The specimens were previously dried in an oven (CIENLAB - CE 220/100) at 110 ± 5 °C for 24 h.

Although basalt powder generated in the basaltic rock extraction process is not considered a waste, it is recommended to evaluate the environmental impact of its use as well as the materials obtained from it, since it is a by-product. The evaluation of the environmental risk was carried out based on ecotoxicological data and environmental concentrations of the material. In this characterization, *Lactuca sativa* L. (lettuce) and *Allium cepa* L. (onion) were used. Bioindicators are testing organisms that, in contact with a material, can generate environmental changes.

Thus, it can be verified whether the basalt powder is properly immobilized (Calmon, 2007) in the cement matrix. These tests were performed with samples of basalt powder and pressed specimens, prepared according to NBR 10006 (ASSOCIAÇÃO BRASILEIRA DE NORMAS TÉCNICAS, 2004). The statistical analysis of variance (ANOVA) complemented with Dunnett's post-tests was used and performed in the GraphPad Prism 5.0 software. Reliability for toxicity is plotted and guided by the number of asterisks, as shown in Table 2.

Table 2 - Statistical parameters according to Dunnett's tests.

Parameter (*)	P	Reliability (%)
*	$p < 0.05$	95
**	$p < 0.01$	99
***	$p < 0.001$	99.9
****	$p < 0.0001$	99.99

The *Allium cepa* L. provides the reactions of the toxic and genotoxic effects of an environmental contaminant such as: bioaccumulation of contaminants in the roots, inhibition of root growth and inhibition of seed germination (Andrade *et al.*, 2010; Bortolotto *et al.*, 2017). To perform this test, 6 onions were prepared for each sample tested, cutting the old root attached to the onion dish and retreated

the outer shells that were dry, without hurting them. Soon, 50 mL of effluent was added from the samples in a 50 mL Falcon tube filling up to the top edge and placed the onion with the root touching the sample. For control, mineral water was used in one group in place of effluent. They were left at room temperature and in the dark for 7 days, and every 24 h sample replacement occurred in the

tubes. After 7 days, all new roots were carefully removed, with the aid of a scalpel, measuring the number of roots that grew, their lengths and the biomass of each one. With an electronic analytical balance (Bioprecisa, model FA-2104N; accuracy of 0.0001 g), the mass of all roots was obtained. The same procedure was performed with samples submitted to mineral water with pH 6-7, for control,

determined with the use of universal pH tape MColorpHast.

Lactuca sativa L. is among the test organisms used to evaluate phytotoxicity, caused by elements in soils that are potential pollutants (Andrade *et al.*, 2010; Bortolotto *et al.*, 2017). In this test, a filter paper disc 8 cm in diameter

was cut and placed inside the Petri dish. Ten lettuce seeds were inserted in each plate, covering the Petri dish with the lid and keeping them stored in a dark place and at room temperature for 72 h. After this period, the number of germinated seeds were verified. The length of the root and stem were measured with a

digital caliper (Caliper 150 mm; accuracy of 0.01 mm). The same procedure was performed with the specimens treated with mineral water for control. This water was at pH between 6 and 7. If not, hydrochloric acid 0.1 mol should be used for this adjustment, determined using MColorphast universal pH tape.

3. Results and discussion

3.1 Characterization of basalt powder

The results of particle size distribution of basalt and sand are shown in Figure 1.

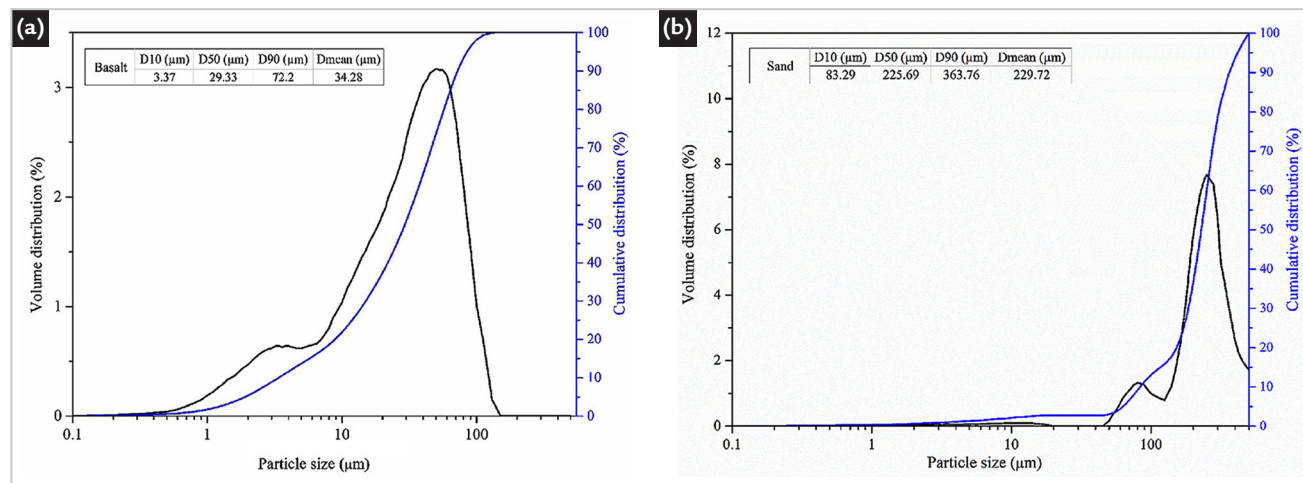


Figure 1 - Particle size distribution of basalt powder (a) and sand (b).

The particle size distribution plots present in practice a monomodal distribution. Basalt presents a mean particle size of 34.28 μm, while sand presents 229.72 μm. Although the mean particle size of sand and basalt are very different, this work does not intend to evaluate the effect of the mean particle size on the mechanical behavior, but the possibility of substituting a com-

mercial sand by an as-received by-product.

The chemical composition of basalt is presented in Table 3. As Table 3 shows, basalt is mainly formed by silicon and aluminum, elements common in ceramic compositions. These elements are combined into crystalline phases, which were determined by XRD (Figure 2), which shows the presence of the main

identified crystalline phases, Anorthite ($\text{CaAl}_2\text{Si}_2\text{O}_8$, JCPDS card 20-0020), Augite ($(\text{Ca},\text{Na})(\text{Mg},\text{Fe},\text{Al},\text{Ti})\text{Si}_2\text{O}_6$, JCPDS card 24-203), and Vermiculite ($(\text{MgFe},\text{Al})_3(\text{Al},\text{Si})_4\text{O}_{10}(\text{OH})_2 \cdot 4\text{H}_2\text{O}$, JCPDS card 16-0613). This is in agreement with Mendes (2016), which identified the crystalline phases Albite, Anorthite, Augite, and Labradorite in the investigated basalt.

Table 3 - Chemical analysis (wt.%) of Basalt by XRF.

Al_2O_3	SiO_2	CaO	Fe_2O_3	K_2O	MgO	MnO	Na_2O	P_2O_5	TiO_2
18.03	52.01	10.90	9.35	0.70	4.08	0.14	3.14	0.30	1.28

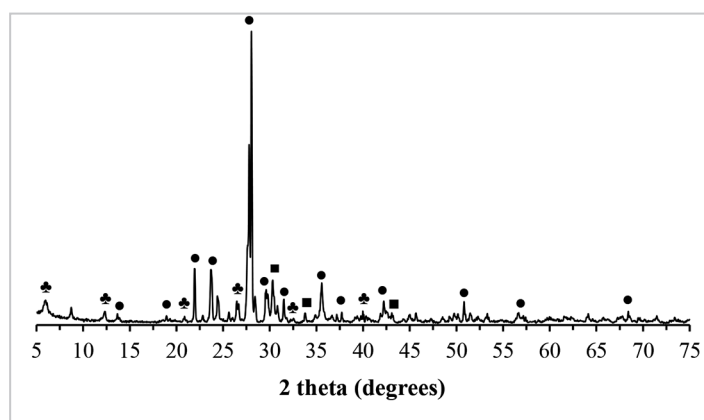


Figure 2 - XRD pattern of basalt powder: ● Anorthite, ▲ Vermiculite, ■ Augite.

3.2 Definition of the Cement: aggregate mass ratio

The results of BS as a function of the specific pressures are presented in Table 4. Table 4 shows that BS is practically invariable with specific pressure and decreases with increasing basalt content.

Table 3 - Chemical analysis (wt.%) of Basalt by XRF.

Cement: aggregate mass ratio	BS (MPa)			
	P _{esp} of samples PRE (MPa)			MOL
	25.5	28.0	30.5	
1:5	3.44 ± 0.17	3.41 ± 0.17	3.39 ± 0.18	2.82 ± 0.18
1:6	3.07 ± 0.13	3.16 ± 0.11	3.18 ± 0.11	-
1:7	2.31 ± 0.14	2.35 ± 0.18	2.38 ± 0.18	-

From these results, the 1:6 cement:aggregate mass ratio and 25.5 MPa of specific pressure (BS of 3.07 ± 0.13 MPa) were chosen to prepare specimens for the next step. This value is higher than that of MOL specimens (2.82 ± 0.18 MPa) and higher than the limit established by the NBR 15310 (ASSOCIAÇÃO BRASILEIRA DE NORMAS TÉCNICAS, 2009b), where the minimum load must be 1000 N (1.0 MPa) for flat fitting tiles and 1300 N (1.3 MPa) for composite fitting tiles; according to standard NBR 13858 (ASSOCIAÇÃO BRASILEIRA DE NORMAS TÉCNI-

CAS, 2009a), the minimum load must be 2500 N (2.5 MPa) for concrete roofing tiles. In addition, this cement:aggregate mass ratio allows to use a larger amount of basalt powder.

The effect of the cement:aggregate mass ratio (trace) and specific pressure on BS is confirmed through the analysis of variance (ANOVA) presented in Table 5.

Based on the analysis of variance of ANOVA for these experimental conditions and with 95% confidence, the value of R² is 0.997 and the adjusted R² is 0.988. The specific pressure (MPa) and the interaction between the two factors do

not have significant statistical influence. This is also clear in Figure 3, which shows the response surface plot of the BS of the tested samples. This figure also shows that there is a small effect of specific pressure on the BS, so that the higher the specific pressure, the higher the BS. In addition, the choice of the 1:6 cement:aggregate mass ratio and the specific pressure of 25.5 MPa represent higher consumption of the alternative material (basalt powder) and lower energy expenditure. Thus, lower operational cost could be obtained to produce flat pressed roofing tiles in relation to commercial material (reference).

Table 5 - Analysis of variance of BS.

Factor	SQ	v	MQ	F	p-test
(1) P _{esp} (MPa)	0.003	1	0.003	0.49	0.610
(2) Cement: aggregate mass ratio	1.974	1	1.974	322.28	0.035
P _{esp} x cement: aggregate mass ratio	0.003	1	0.003	0.49	0.610
Error	0.006	1	0.006		
SQ Total	1.986	4			

SQ = sum of squares; v = variance (degrees of freedom); MQ = quadratic mean; F = Fischer test; p-test = reliability test.

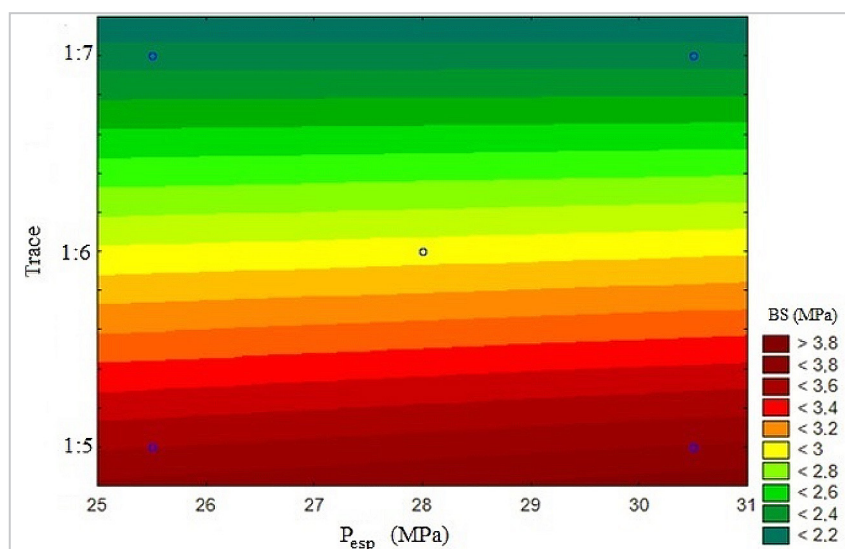


Figure 3 - Response surface plot of BS.

3.3 Evaluation of the effect of curing time on the bending strength

The crystalline phases of the MOL and PRE specimens obtained at 7 days of curing are shown in the Figure 4.

Figure 4 shows that the predominant phase of MOL samples is Alite at 7days,

but Quartz and Belite are also present. The majority phase of PRE samples is Anorthite at 7 days due to the addition of basalt. Augite and Hydrated calcium silicate are also present. Usually, the pres-

ence of Anorthite increases the mechanical strength and chemical stability of the material (Rouabhia *et al.*, 2018). These structural features interfere in porosity, Figure 5.

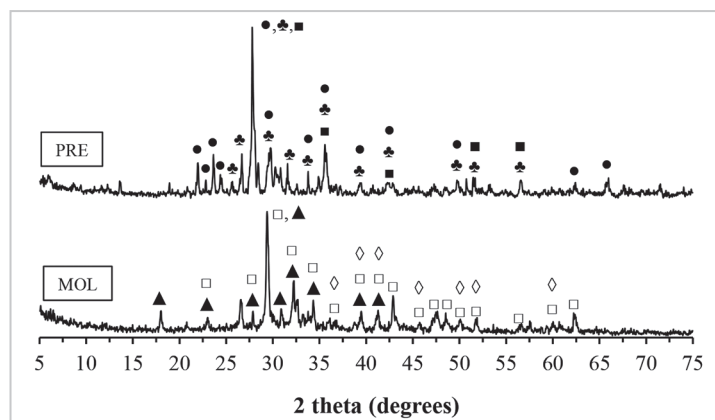


Figure 4 - XRD patterns of MOL and PRE specimens at 7 days of curing:
● Anorthite, ◐ Hydrated calcium silicate, ■ Augite, ◇ Quartz, □ Alite, ▲ Belite.

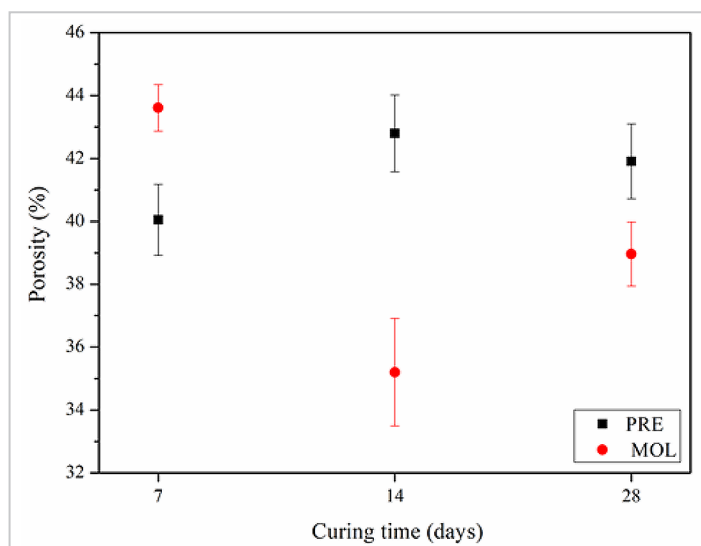


Figure 5 - Porosity of the studied samples.

Although at 7 days of curing the PRE samples presented lower porosity than the MOL samples, at 14 and 28 days of curing the latter showed lower porosity. Possibly the mixture has achieved adequate packaging of the particles in the conformation with basalt in the granulometry used (as received).

Eugênio *et al.* (2021) evaluated the effect of using iron ore tailing (IOT) on the porosity of concrete roof tiles obtained by the extrusion process. They used the base mass ratio consisted of 1:3:0.56 (cement:medium grade natural sand:limestone powder) and the treatments were based on 25, 50, 75, and 100% mass replacement of limestone powder by iron ore tailings. They obtained a porosity of, approximately, 13% at 28 days curing time. Their higher amount

of Portland cement can explain their less porosity related to our cement:aggregate mass ratio (1:6). The higher porosity of PRE specimens has a direct influence on mechanical strength, as will be seen later.

The microstructural evolution of MOL and PRE samples cured at 7, 14, and 28 days, performed by SEM, is shown in Figure 6. Figure 6 shows the increased formation of the Hydrated calcium aluminum sulfate or Ettringite phase (C₆A₃H₃2) with increased curing time. This crystalline phase has a column structure and is mainly responsible for the mechanical strength in cementitious materials. Mehta *et al.* (2008) explain that Ettringite is the first product to crystallize during the initial hours of hydration at room temperature, contributing to the handle and the development of initial

strength. Under appropriate conditions, soluble sulfates, added in gypsum form in the final stage of cement manufacturing, dissolve rapidly and react with Tricalcium aluminate (C₃A), precipitating in the form of Ettringite (Odler, 2007).

The presented structural and microstructural aspects directly interfere in the mechanical behavior of the samples. The results of BS of MOL and PRE specimens at 7, 14, and 28 days of curing are shown in Figure 7. This figure shows that the BS increases with the increase of curing time, regardless of the type of conformation employed. However, the PRE specimens present higher BS than MOL specimens, even presenting higher porosity.

Here, two important factors that influence on BS should be considered:

i) the highest porosity of PRE specimens in relation to MOL specimens; and ii) the highest amount of aggregate in the PRE specimens (cement:aggregate mass ratio of 1:6) in relation to MOL specimens (cement:aggregate mass ratio of 1:5).

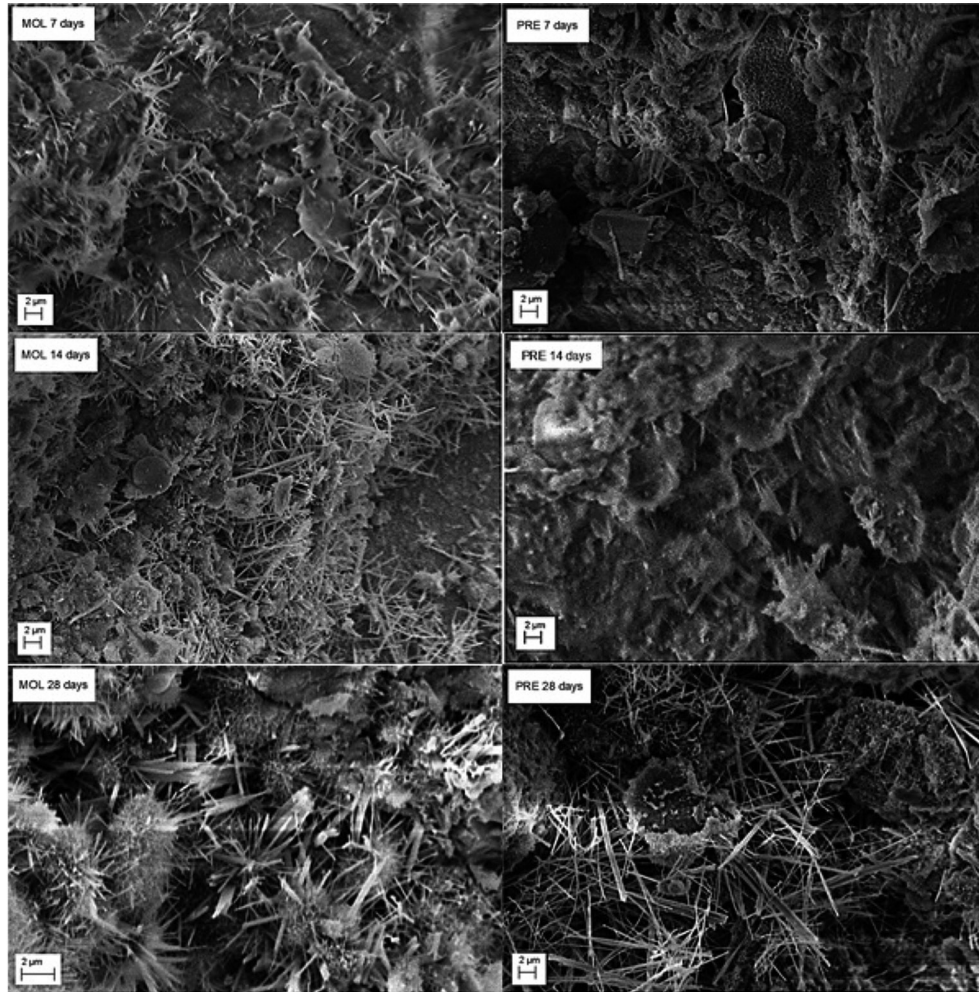


Figure 6 - Micrographs (SEM) of MOL and PRE specimens at 7, 14, and 28 days of curing.

These two factors should promote the reduction of BS of PRE specimens in relation to MOL specimens. However, this is not observed in Figure 7. It is possible that there occurred a better interaction between the cementitious matrix and ba-

salt particles than with the sand particles, acting more efficiently as structural reinforcement and hence increasing BS. Sam *et al.* (2020) obtained values of bending strength varying from 1 to 8.5 MPa depending on the waste engine-vegetable oil

ratio as binder in roofing tiles. Menezes *et al.* (2010) studied the use of electro-fused alumina production waste in ceramic bricks and roof tiles fired at 1000 °C for ceramic bricks and roof tiles and obtained a modulus of rupture of 6.5 MPa.

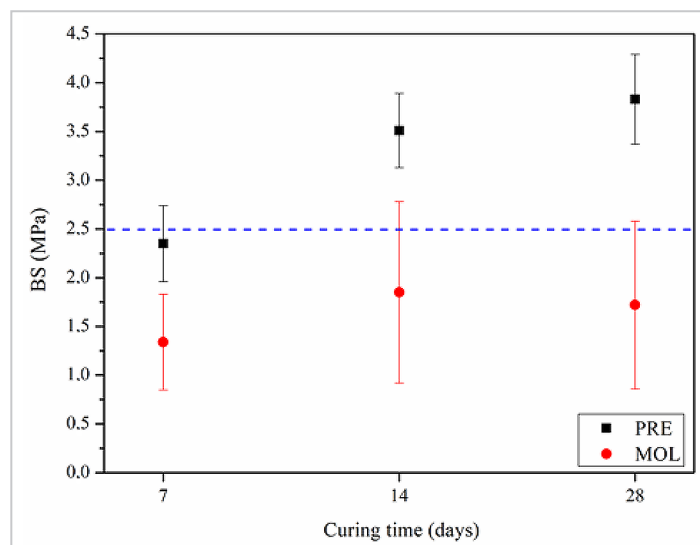


Figure 7 - BS of MOL and PRE specimens at 7, 14, and 28 days of curing.

3.4 Technological and toxicological characterization

Table 6 shows the water absorption (AA) results of the specimens at 28 days of curing.

Table 6 - Results of water absorption (AA) of the specimens at 28 days of curing.

Description	Absorption of water (%)
PRE	19.96 ± 0.94
MOL	15.25 ± 0.88

It is observed that the PRE samples met the specifications of NBR 15310 (ASSOCIAÇÃO BRASILEIRA DE NORMAS TÉCNICAS, 2009c), which defines that AA should be less than 20%. Apparently, the MOL specimens achieved better densification in the conformation and curing stage and presented lower AA values.

Eugênio *et al.* (2021) obtained AA of, approximately, 6.7% for a mass ratio of 1:3:0.56 (cement:medium grade natural sand:limestone powder), probably because of the higher amount of cement Portland related to our cement:aggregate mass ratio (1:6).

To evaluate the environmental impact of basalt use, ecotoxicity tests were performed using 10 samples for *Lactuca sativa* L. (lettuce) and 6 for *Allium cepa* L. (onion).

Figure 8 shows the results of number of roots, biomass, and root sizes of *Allium cepa* L. samples for the control group, basalt powder and PRE specimens.

Using variance analysis (ANOVA), a statistical analysis was performed, complemented with Dunnett's post-tests and with the aid of Graphpad Prism 5.0 software. In cases "a" and "b", it is observed that basalt powder presents toxicity with reliability of

95% (presence of one asterisk on the Basalt bar). Although the root growth in basalt samples is smaller than control samples, they are within acceptable range.

In case "c", none of the basalt powder specimens was toxic due to the absence of asterisk on the bars. In these cases, it is observed that the PRE specimens present toxicity with reliability of 99.9%, represented by the asterisks above the bars. That is, the toxicity of PRE specimens does not occur due to the presence of basalt, but due to cement. Although they have a smaller growth than the control group, they are within the acceptable variation.

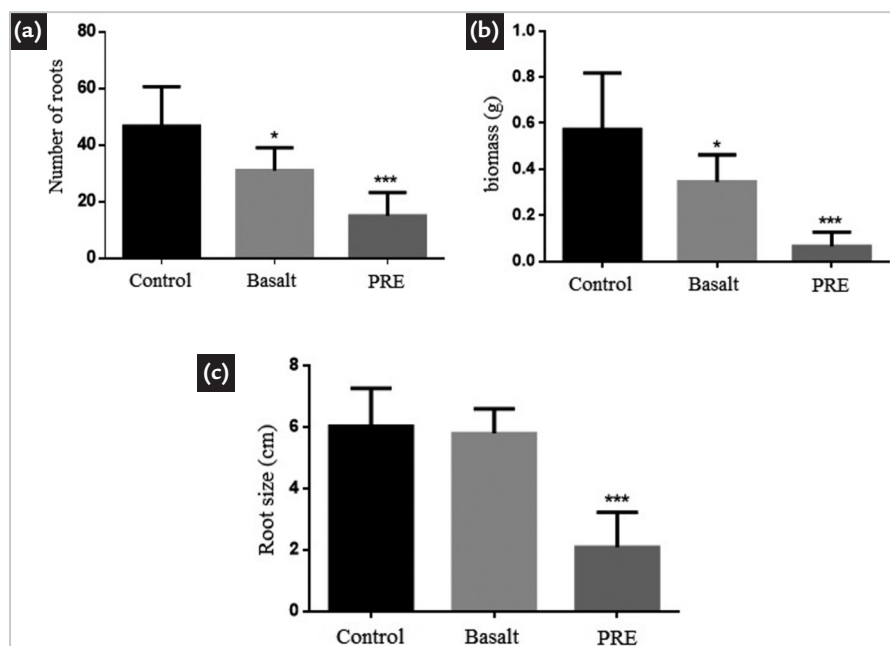


Figure 8 - Subchronic toxic effects of effluents in bulbs of *Allium cepa* L. in terms of: a) number of roots, b) biomass, and c) root size.

Figure 9 shows the results of root size, hypocotyl size, and radicle size of the *Lactuca sativa* L. samples for the control group, basalt powder and PRE specimens. Figure 9 shows that basalt powder does not present toxicity in any of the specimens (absence of asterisks on basalt bars). In cases "a" and "c", the result of the bars shows behavior very close to the control and different from case "b", in which basalt powder was above the Control, that is, with no toxicity higher than the Control.

The PRE specimens (case "b") do not present toxicity (absence of asterisk on the bar) because of a higher growth of the roots compared to the control, as demonstrated by the values represented by the bars. On the other hand, the PRE specimens of cases "a" and "c" present toxicity with reliability of 95 and 99%, respectively, represented by asterisks: however, they are within the acceptable range.

It can be concluded that the composition used in the specimens, containing

cement and basalt powder, is not toxic, confirming the possibility of total replacement of sand by basalt powder.

In addition to this, one can also mention the most effective control of the manufacturing process promoted by the powder technology, since it represents a reduction of operational production costs, through automation, reduction of labor and quality improvement, and reduction of the environmental impact by replacing a raw material (sand) by an industrial by-product.

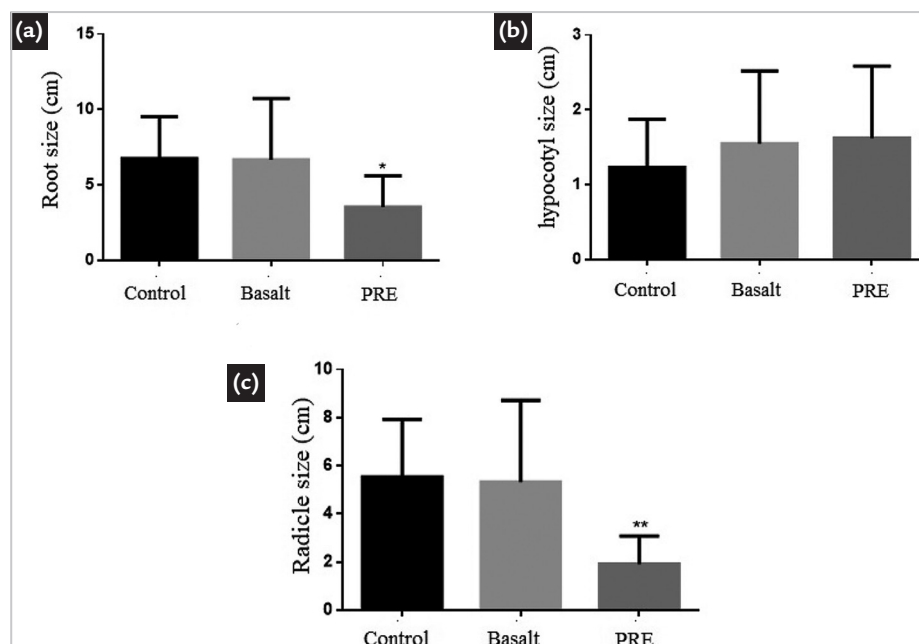


Figure 9 - Subchronic toxic effects of effluents in *Lactuca sativa* L. seeds in terms of: a) root size, b) hypocotyl size, and c) radicle size.

4. Conclusions

In this article, experimental results were presented of the development of pressed flat plate from powder technology, based on cementitious material and basalt powder in substitution to sand, for application in building roofs (tile). In all pressed samples (PRE specimens), the increase in curing time (7, 14, and 28 days) led to an increase in bending strength, reaching 3.9 MPa with a 1:6 cement:aggregate mass ratio compared

to the value of 1.8 MPa obtained for the molded samples (MOL specimens) with a 1:5 cement:aggregate mass ratio, even with higher porosity than MOL specimens. Water absorption (AA) at 28 days was $19.96 \pm 0.94\%$ in PRE specimens and $15.25 \pm 0.88\%$ in MOL specimens, both lower than the value of 20% established in NBR 13858:2. In the ecotoxicity tests to evaluate the impact of basalt use on cement-based

artifacts, the obtained material presented non-toxic and non-hazardous behavior. Thus, the use of basalt, in substitution of sand for the production of roofing tiles through powder technology, represents a reduction of operational production costs, through automation, reduction of labor and quality improvement, and reduction of the environmental impact by replacing a raw material (sand) by an industrial by-product.

Acknowledgments

The authors are very grateful to Coordenação de Aperfeiçoamento de Pessoal de Nível Superior (CAPES/Brazil;

process n. 88887.356784/2019-00) and Conselho Nacional de Desenvolvimento Científico e Tecnológico (CNPq/

Brazil; process n. 308669/2016-9, process n. 307761/2019-3, and process n. 306177/2015-3) for supporting this work.

References

- ABRAHAM, D. P. R.; JOSEPH, A.; JASHEELA, A.; BINURAJ, P. R.; SARMA, J. Development of coir-fibre cement composite roofing tiles. *Procedia Technology*, v. 24, p. 169-178, 2016. DOI 10.1016/j.protcy.2016.05.024.
- ANDRADE, L. F.; DAVIDE, L. C.; GEDRAITE, L. S. The effect of cyanide compounds, fluorides, aluminum, and inorganic oxides present in spent pot liner on germination and root tip cells of *Lactuca sativa*. *Ecotoxicology and Environmental Safety*, v. 73, n. 4, p. 626-631, 2010. DOI: <https://doi.org/10.1016/j.ecoenv.2009.12.012>.
- ASSOCIAÇÃO BRASILEIRA DE NORMAS TÉCNICAS. *ABNT NBR 5733/1991*: Cimento Portland de alta resistência inicial. Rio de Janeiro: ABNT, 1991.
- ASSOCIAÇÃO BRASILEIRA DE NORMAS TÉCNICAS. *ABNT NBR 10006*: Procedimento para obtenção de extrato solubilizado de resíduos sólidos. Rio de Janeiro: ABNT, 2004.
- ASSOCIAÇÃO BRASILEIRA DE NORMAS TÉCNICAS. *ABNT NBR 13858:2/2009*: Telhas de concreto - Parte 2 : requisitos e métodos de ensaio. Rio de Janeiro: ABNT, 2009.
- ASSOCIAÇÃO BRASILEIRA DE NORMAS TÉCNICAS. *ABNT NBR 15310/2009*: Componentes cerâmicos - Telhas - terminologia, requisitos e métodos de ensaio. Rio de Janeiro: ABNT, 2009.
- ASSOCIAÇÃO BRASILEIRA DE NORMAS TÉCNICAS. *ABNT NBR 15900:1/2009*: Água para amassamento do concreto. Parte 1: requisitos. Rio de Janeiro: ABNT, 2009.
- ASSOCIAÇÃO BRASILEIRA DE NORMAS TÉCNICAS. *ABNT NBR 12142/2010*: Concreto - Determinação da

- resistência à tração na flexão de corpos de prova prismáticos. Rio de Janeiro: ABNT, 2010.
- ASSOCIAÇÃO BRASILEIRA DE NORMAS TÉCNICAS. **ABNT NBR 7215/2019**: Cimento Portland - determinação da resistência à compressão de corpos de prova cilíndricos. Rio de Janeiro: ABNT, 2019.
- BORTOLOTO, T.; SILVA, J.; SANTANA, A. C.; TOMAZI, K. O.; GEREMIAS, R.; ANGIOLETTO, E.; PICH, C. T. Evaluation of toxic and genotoxic potential of a wet gas scrubber effluent obtained from wooden-based biomass furnaces: a case study in the red ceramic industry in southern Brazil. *Ecotoxicology and Environmental Safety*, v. 143, p. 259-265, 2017. DOI: <https://doi.org/10.1016/j.ecoenv.2017.05.033>.
- BRASILEIRO, L. L.; MATOS, J. M. E. Revisão bibliográfica: reutilização de resíduos da construção e demolição na indústria da construção civil. *Cerâmica*, v. 61, N. 358, p. 178-189, 2015. DOI: <https://doi.org/10.1590/0366-69132015613581860>.
- CABRAL JUNIOR, M.; AZEVEDO, P. B. M.; CUCHIERATO, G.; MOTTA, J. F. M.; Estudo estratégico da cadeia produtiva da indústria cerâmica no estado de São Paulo: Parte II – indústria de revestimentos. *Cerâmica Industrial*, v. 24, n. 2, p. 13-21, 2019. DOI: <https://doi.org/10.4322/cerind.2019.010>.
- CALMON, J. L. Resíduos industriais e agrícolas. In: ISAIA, G. C. (ed.). *Materiais de construção civil e princípios de ciência e engenharia de materiais*. São Paulo: IBRACON, 2007. p. 1583-1622.
- COTA, F. P.; MELO, C. C. D.; PANZERA, T. H.; ARAÚJO, A. G.; BORGES, P. H. R.; SCARPA, F. Mechanical properties and ASR evaluation of concrete tiles with waste glass aggregate. *Sustainable Cities and Society*, v. 16, p. 4956, 2015. DOI: <http://dx.doi.org/10.1016/j.scs.2015.02.005>.
- DAMASCENO, F. A.; MACEDO, O. A. P.; OLIVEIRA, J. L.; OLIVEIRA, C. A. E.; BRANDÃO, L. F. Propriedades físicas, mecânicas e térmicas de telhas de concreto fabricadas com adição de diferentes materiais isolantes. *Engenharia na Agricultura*, v. 23, n. 5, p. 406-417, 2015. DOI: <https://doi.org/10.13083/reveng.v23i5.578>.
- DESTEFANI, A. Z.; HOLANDA, J. N. F. Utilização do planejamento experimental em rede simplex no estudo de resíduo de rocha ornamental como filler para obtenção de máxima compacidade. *Cerâmica*, v. 57, n. 344, p. 491-498, 2011. DOI: <https://doi.org/10.1590/S0366-69132011000400018>.
- EUGÊNIO, T. M. C.; FAGUNDES, J. F.; VIANA, Q. S.; VILELA, A. P.; MENDES, R. F. Study on the feasibility of using iron ore tailing (iot) on technological properties of concrete roof tiles. *Construction and Building Materials*, v. 279, p. 122484, 2021. DOI: <https://doi.org/10.1016/j.conbuildmat.2021.122484>.
- KOPPE, A.; GUINDANI, E. N.; MANCIO, M. Avaliação do potencial de resíduo de rochas basálticas como matéria-prima para a produção de cimentos alternativos: processo de álcali-ativação. *Revista de Arquitetura IMED*, v. 4, n. 2, p. 24-32, 2015. DOI: <https://doi.org/10.18256/2318-1109/arqimed.v4n2p24-32>.
- MEHTA, P. K.; MONTEIRO, P. J. M.; HELENE, P. R. L.; PAULON, V. A. *Concreto*: microestrutura, propriedades e materiais. 2. ed. São Paulo: IBRACON, 2008.
- MENDES, T. M.; GUERRA, L.; MORALES, G. Basalt waste added to Portland cement. *Acta Scientiarum. Technology*, v. 38, n. 4, p. 431-436, 2016. DOI: <https://doi.org/10.4025/actascitechnol.v38i4.27290>.
- MENEZES, R. R.; MARQUES, L. N.; SANTANA, L. N. L.; KIMINAMI, R. H. G. A.; NEVES, G. A.; FERREIRA, H. S. Uso de resíduo da produção de alumina eletrofundida na produção de blocos e telhas cerâmicos. *Cerâmica*, v. 56, n. 339, p. 244-249, 2010. DOI: <https://doi.org/10.1590/S0366-69132010000300006>.
- ODLER, I. Hydration, setting and hardening of Portland cement. In: HEWLETT, P. C. (ed.). *Lea's chemistry of cement and concrete*. China: Butterworth-Heinemann, 2007. p. 241-298.
- ROUABHIA, F.; NEMAMCHA, A.; MOUMENI, H. Elaboração e caracterização de cerâmicas porosas de multianortita-albita preparadas a partir de caulim argelino. *Cerâmica*, v. 64, n. 369, p. 126-132, 2018. DOI: [https://doi.org/10.1061/\(ASCE\)MT.1943-5533.0004078](https://doi.org/10.1061/(ASCE)MT.1943-5533.0004078).
- SAM, S. S.; HABIB, N. Z.; AUN, N. C.; YONG, C. S.; BASHIR, M. J. K.; PING, T. W. Blended waste oil as alternative binder for the production of environmental friendly roofing tiles. *Journal of Cleaner Production*, v. 258, p. 120937, 2020. DOI: <https://doi.org/10.1016/j.jclepro.2020.120937>.
- SANTANA, J. A.; FERREIRA, E. A. M. The influence of the amount of the powdery materials level in the crushed rock residues, in the concrete resistances in the first ages. In: SIMPÓSIO EPUSP SOBRE ESTRUTURAS DE CONCRETO, 6., 2006, São Paulo. *Anais [...]*. São Paulo: [S. n.], 2006. p. 17-32. ISBN 85-86686-36-0 2006.
- SILVA, K. R.; JESUS, F. B. T.; INOCENTE, J. M.; ARCARO, S.; PEREIRA, F. R.; MONTEDO, O. R. K. Basalt-containing pressed cement plates for construction systems: technological and toxicological characterization. *Journal of Materials in Civil Engineering*, v. 34, p. 04021443-1-04021443-11, 2022. DOI: [https://doi.org/10.1061/\(ASCE\)MT.1943-5533.0004078](https://doi.org/10.1061/(ASCE)MT.1943-5533.0004078).
- SOUZA, D. M.; LAFONTAINE, M.; CHARRON-DOUCET, F.; BENGUA, X.; CHAPPERT, B.; DUARTE, F.; LIMA, L. Comparative life cycle assessment of ceramic versus concrete roof tiles in the Brazilian context. *Journal of Cleaner Production*, v. 89, p. 165-173, 2015. DOI: <http://dx.doi.org/10.1016/j.jclepro.2014.11.029>.

Received: 19 May 2021 - Accepted: 20 June 2022.



All content of the journal, except where identified, is licensed under a Creative Commons attribution-type BY.